



## Effects of ultrasonic treatment on microstructure and mechanical properties of Mg–6Zn–0.5Y–2Sn alloy

Han-song XUE<sup>1,2</sup>, Zhi-hui XING<sup>1</sup>, Wei-na ZHANG<sup>1</sup>, Gang YANG<sup>1</sup>, Fu-sheng PAN<sup>1,2</sup>

1. School of Materials Science and Engineering, Chongqing University, Chongqing 400044, China;

2. National Engineering Research Center for Magnesium Alloys, Chongqing University, Chongqing 400044, China

Received 14 July 2015; accepted 19 October 2015

**Abstract:** The effects of the ultrasonic treatment on the microstructure and mechanical properties of Mg–6Zn–0.5Y–2Sn alloy were investigated. The results show that the ultrasonic treatment has significant effect on the microstructure and mechanical properties of Mg–6Zn–0.5Y–2Sn alloy. The phases in Mg–6Zn–0.5Y–2Sn alloy are  $\alpha$ -Mg, MgZn<sub>2</sub>, MgSnY, Mg<sub>2</sub>Sn, and a small amount of *I*-phase. With the application of ultrasonic treatment, *I*-phase nearly disappears, and with increasing the ultrasonic treatment power, the coarse dendrites gradually change into roundish equiaxed grains. The second phases at the  $\alpha$ -Mg boundaries transform from coarse, semicontinuous and non-uniform to fine, discontinuous, uniform and dispersive. When the ultrasonic treatment power is 700 W, the best comprehensive mechanical properties of Mg–6Zn–0.5Y–2Sn alloy are obtained. Compared with the untreated alloy, the 0.2% tensile yield strength, ultimate tensile strength and elongation are improved by 28%, 30% and 67%, respectively.

**Key words:** Mg–6Zn–0.5Y–2Sn alloy; ultrasonic treatment; microstructure; mechanical properties

### 1 Introduction

Magnesium alloys, as the lightest metallic structure materials, have excellent potentials to be used as structure materials in the aerospace, transportation and mobile electronics industries due to their interesting combination of engineering properties such as low density, high specific strength and stiffness, good damping capacity, excellent machinability and easy recovery [1–4]. However, the applications of magnesium alloy are still limited because its strength and ductility are not good enough for commercial applications [5,6]. Therefore, the wide application of magnesium alloys depends heavily on the development of new high-strength and high-ductility magnesium alloys.

Recently, Mg–Zn–RE (RE=Y, Gd, Er) alloys have attracted great attention due to their good mechanical properties, especially the Mg–Zn–Y alloys, which could form the very efficient *I*-phase (Mg<sub>3</sub>Zn<sub>6</sub>Y). As an icosahedral quasicrystalline structure, the *I*-phase has interesting combination of mechanical properties such as high strength, high temperature plasticity and low

interfacial energy [7–9]. But it is well known that the *I*-phase is extremely brittle at room temperature and this is unfavorable for the elongation of the alloy. More recently, DONG et al [10] and TUREN [11] have found that the as-cast microstructures of AZ64 and AZ91 alloys can be refined and their tensile properties can be improved when 0.5% Sn (mass fraction) was added into the alloys. QI et al [12] reported that Sn can modify the microstructure of magnesium alloys and form Mg<sub>2</sub>Sn phase when the amount of Sn added into the magnesium alloys is appropriate. The Mg<sub>2</sub>Sn phase possesses the superior properties such as the high microhardness, high melting point and thermal stability. As mentioned above, the effects of Sn addition on the microstructure and mechanical properties of Mg–Zn–RE alloy have attracted people's attention and the Mg–Sn–Zn–Y quaternary alloys were investigated [13,14]. The study indicated that the quaternary alloys have superior comprehensive mechanical properties in wide temperature range. This is because the Mg–Sn–Zn–Y quaternary alloys consist of several stable intermetallic compounds, such as MgZn<sub>2</sub>, MgSnY and Mg<sub>2</sub>Sn phases, which can provide strong bonding strength with the matrix [15,16].

**Foundation item:** Project (cstc2015jcyjBX0036) supported by Chongqing Research Program of Basic Research and Frontier Technology, China; Project (51571040) supported by the National Natural Science Foundation of China; Project supported by the Sharing Fund of Chongqing University's Large-scale Equipment, China

**Corresponding author:** Han-song XUE; Tel: +86-23-65111212; E-mail: [hsxue@sohu.com](mailto:hsxue@sohu.com)

DOI: 10.1016/S1003-6326(16)64263-2

Ultrasonic treatment is a simple, clean and effective physical means for modifying the microstructure of the low-melting alloy during the solidification process [17,18]. Ultrasonic treatment has been introduced into light alloys extensively, such as aluminum alloys and magnesium alloys. The previous studies have shown that after ultrasonic treatment, the microstructure of magnesium alloys would become finer, more homogeneous, dispersive, and less segregation [19,20]. More recently, the effects of ultrasonic treatment on the microstructure and mechanical properties of Mg–Zn–RE alloys have been investigated [21]. But few works have been done on the Mg–Zn–RE alloys containing Sn. As mentioned above, the Mg–Sn–Zn–Y quaternary alloys have great potential for commercial applications. However, the alloys are still not good enough for wide use due to the relatively low absolute strength. Therefore, it is necessary to research the effects of the ultrasonic treatment on the microstructure and mechanical properties of these alloys.

Accordingly, in the present work, the effects of ultrasonic treatment on the microstructure and mechanical properties of Mg–6Zn–0.5Y–2Sn alloy were investigated.

## 2 Experimental

The Mg–6Zn–0.5Y–2Sn alloy was treated by a high intensity ultrasonic equipment. Figure 1 shows the schematic diagram of the experimental devices for ultrasonic treatment. The ultrasonic system mainly consists of an ultrasonic generator system with the fixed frequency of 20 kHz and the maximum power of 1 kW, an ultrasonic transducer, an ultrasonic horn and an ultrasonic probe. The ultrasonic probe is made of titanium alloy.

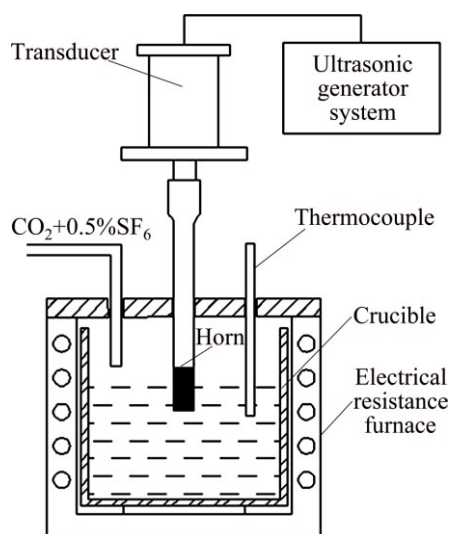


**Fig. 1** Schematic diagram of experimental devices for ultrasonic treatment

Mg–6Zn–0.5Y–2Sn (mass fraction, %) alloy was used as the experimental material. High-purity Mg (>99.9%, mass fraction), Zn (>99.95%), Sn (>99.9%) and Mg–30%Y master alloy were used as raw materials. The alloys were melted in the stainless steel crucible and the melt was protected by CO<sub>2</sub>+0.5%SF<sub>6</sub> (volume fraction) mixed gas. The total mass of the alloy was 1.2 kg. The pure Mg and Mg–30%Y master alloy were first heated, and pure Zn and Sn were added into the alloys when the alloys were melted and the temperature increased to 700 °C, and then the alloys were maintained at 730 °C for 20 min in order to make the alloy element fully homogenized, at last we stop heating and pour the melt into the steel mold. When the temperature of the alloy melt was reduced to 680 °C, the ultrasonic processing was conducted with immersing the ultrasonic probe into the melt at a depth of about 30 mm and the ultrasonic treatment time was 30 s. After the ultrasonic treatment, the ultrasonic probe was removed quickly and the alloy melt was cooled in water. In order to achieve better ultrasonic treatment process, the powers were set as 300, 500 and 700 W, respectively. For comparison, the contrastive sample was also prepared without ultrasonic treatment which was defined as 0 W ultrasonic treatment for convince. The samples were cut from the same location for comparison.

The cast specimens were sectioned, ground, mechanically polished and etched with 4% nitric acid in alcohol to reveal their microstructures. The microstructures of the specimens were observed by an optical metallographic microscope (OM, NEISS NEOPHOT–30) and a scanning electron microscope (SEM, TESCAN VEGA II LMU) equipped with an INCA Energy 350 energy dispersive X-ray spectrometer (EDS, Oxford Inca). Phase component analysis was conducted with a Rigaku D/max 2500PC X-ray diffraction (XRD) using a Cu K<sub>α</sub> radiation with a scanning angle range from 10° to 90° and a scanning rate of 4 (°)/min. The tensile tests were performed at a constant strain rate of 1 mm/min on an electronic universal testing machine (SANS CMT 5105) at room temperature.

## 3 Results and discussion

### 3.1 Microstructure of as-cast alloy

Figure 2 shows the XRD patterns of as-cast Mg–6Zn–0.5Y–2Sn alloy with different ultrasonic treatment powers. In the XRD patterns of Mg–6Zn–0.5Y–2Sn alloy, the  $\alpha$ -Mg, MgZn<sub>2</sub>, I-phase, and Mg<sub>2</sub>Sn phases are marked. Combining the EDS results with the XRD patterns, the phase with the mole ratio of Mg:Sn:Y of roughly 1:1:1 exists in the Mg–6Zn–0.5Y–2Sn alloy. GORNY et al [14] and ZHAO et al [15] have been

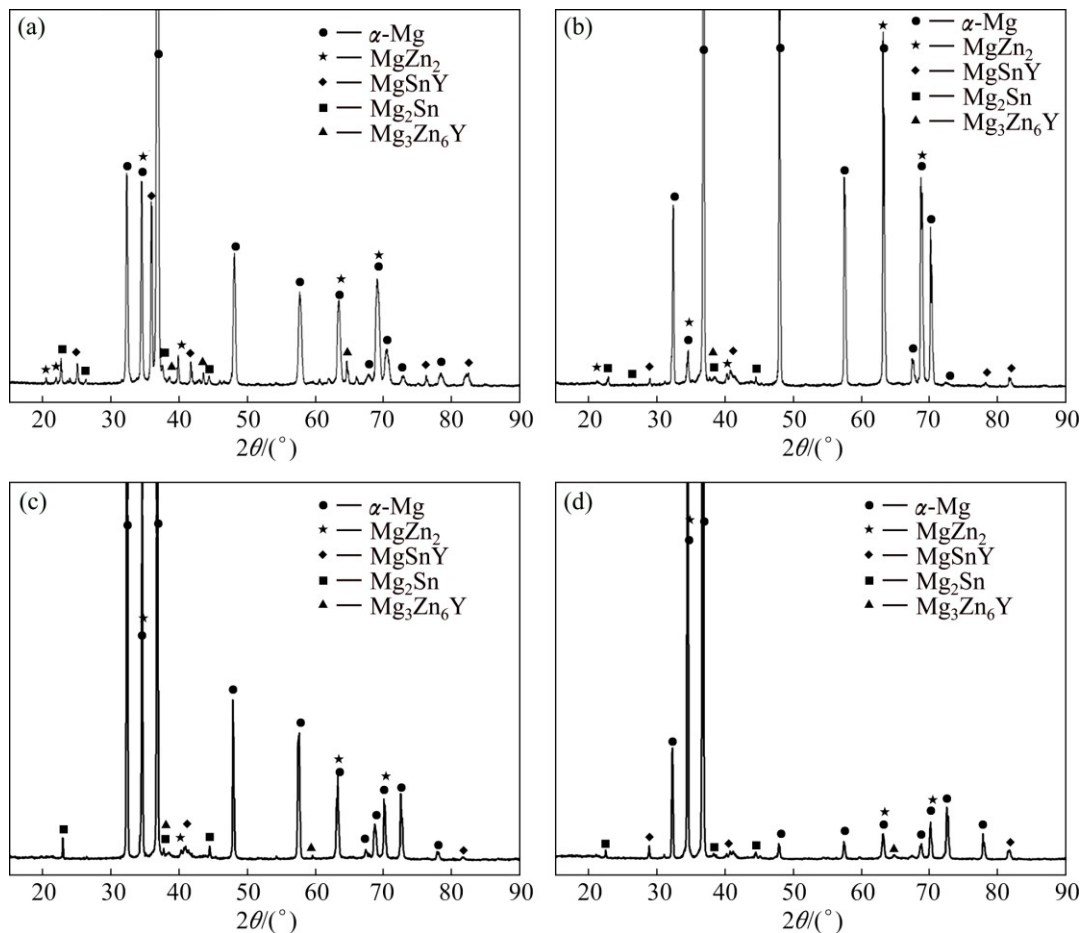


**Fig. 2** XRD patterns of as-cast Mg-6Zn-0.5Y-2Sn alloy with different ultrasonic treatment powers: (a) 0 W; (b) 300 W; (c) 500 W; (d) 700 W

reported that this phase is MgSnY phase. Therefore, the residual peaks of the XRD patterns are indexed as the MgSnY phase. As shown in Fig. 2, it can be indicated that the phase compositions of the alloys are mainly composed of primary  $\alpha$ -Mg, MgZn<sub>2</sub>, Mg<sub>2</sub>Sn, MgSnY, and a small amount of I-phase, which indicates that ultrasonic treatment does not change the phase constituent of the alloy. However, the diffraction peaks of MgZn<sub>2</sub>, MgSnY and Mg<sub>2</sub>Sn phases of the alloy with ultrasonic treatment are weakened compared with those of the untreated alloy, which indicates that the amount of these phases decreases. It can be indicated that the ultrasonic treatment is helpful for solid solution of the second phase into the  $\alpha$ -Mg matrix. After the ultrasonic treatment, the second phase dissolves into the  $\alpha$ -Mg matrix significantly, especially the small amount of I-phase nearly all dissolves into the  $\alpha$ -Mg matrix.

Figure 3 shows the optical images of as-cast microstructures of the alloys with different ultrasonic treatment powers. As shown in Fig. 3(a), without ultrasonic treatment, the primary  $\alpha$ -Mg matrix of the alloy is non-uniform, and the coarse dendritic structure

exists in the alloy. Figures 3(b)–(d) show the microstructures of the alloys which were applied 300, 500 and 700 W ultrasonic treatments, respectively. With the application of the ultrasonic treatment, the coarse dendritic structure is broken into roundish one, and with increasing the ultrasonic treatment power, the grains become more roundish which demonstrates that the dendrite growth mode gradually transforms to roundish equiaxed grain growth mode. With the application of 300 W ultrasonic treatment, the primary  $\alpha$ -Mg matrix exhibits the nearly petal shaped grain structure, and with increasing the ultrasonic treatment power to 500 W, the primary  $\alpha$ -Mg matrix exhibits the nearly equiaxed grain structure, which indicates that a better microstructure is achieved after ultrasonic treatment. When the ultrasonic treatment power attains to 700 W, the coarse dendrites microstructure is broken and changes into roundish equiaxed grains.

It is clear that ultrasonic treatment has an observable effect on improving the microstructure of Mg-6Zn-0.5Y-2Sn alloy due to the cavitation effect and acoustic steaming of the ultrasonic treatment. From

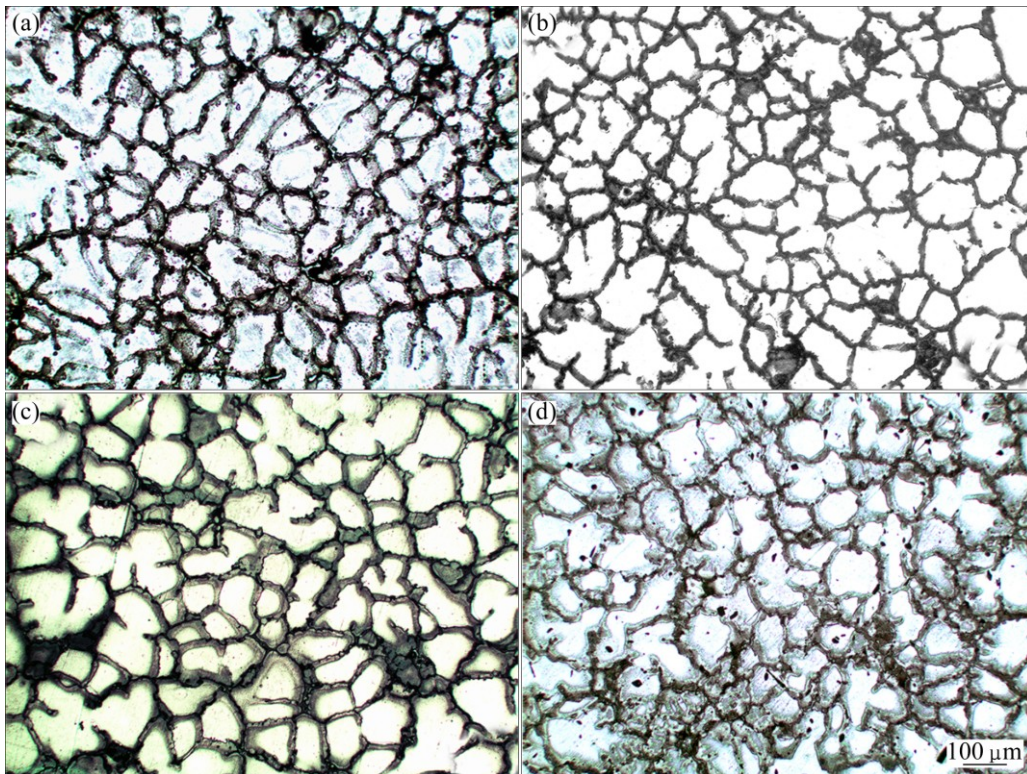


**Fig. 3** Optical images of as-cast microstructures of alloys with different ultrasonic treatment powers: (a) 0 W; (b) 300 W; (c) 500 W; (d) 700 W

the previous studies, it is well known that ultrasonic cavitation occurs in melt near the surface of the ultrasonic radiator/horn interface when the high-intensity ultrasonic treatment is introduced into melted alloy [18,22,23]. What is more, with the application of ultrasonic treatment, a large number of cavitation bubbles form due to the fact that the melt is subjected to local tension stresses and further pulled cracks, and the number of the cavitation bubbles increases with increasing the ultrasonic power. The volume of the cavitation bubbles increases during the growth of the cavitation bubbles, while their internal pressure decreases. The temperature in the cavitation bubbles becomes lower and thus the temperature of cavitation bubbles/melt interface becomes lower too, which causes undercooling and it is needed for heterogeneous nucleation of solid phase locally [23]. The cavitation bubbles continue to expand and finally collapse at a very high speed, causing high instantaneous temperature and pressure in the melt. The high instantaneous pressure makes the dendrites fragmentize and then subsequently spread into the melt to form new grains. Furthermore, the collapse of cavitation bubbles induces high speed flow in the melt which is favorable to decreasing the solute enrichment in front of the solidification, thus, the effect of constitutional undercooling reduces, which results in that the  $\alpha$ -Mg grains grow up consistently in all

directions and form nearly equiaxial grain structure.

The low and high magnifications SEM images of the as-cast microstructures of alloys with different ultrasonic treatment powers are shown in Figs. 4 and 5, respectively. In Fig. 5, the second phases are identified by combining the XRD patterns (Fig. 2) with the EDS analysis (Figs. 5(e)–(f)). Figures 4(a) and 5(a) show that the as-cast microstructure of Mg–6Zn–0.5Y–2Sn alloy without ultrasonic treatment consists of some coarse semicontinuous net MgZn<sub>2</sub>, MgSnY, and Mg<sub>2</sub>Sn phases, which are mainly distributed at the grain boundaries. However, after 300 W ultrasonic treatment, the morphologies of the coarse semicontinuous net phases do not change obviously because of small ultrasonic power. When the ultrasonic treatment power increases to 500 W, the microstructures of the coarse semicontinuous net phases become fine, discontinuous and uniform. Especially, at the power of 700 W, the coarse, semicontinuous net phases change into nearly fine, uniform, and dispersive particles which can provide strong bonding with the matrix and are beneficial to dispersion strengthening. In addition, although the peaks of the Mg<sub>2</sub>Sn phase exist in the XRD pattern of the alloy with the ultrasonic treatment power of 700 W, the compound is not observed in Figs. 4 and 5, which is possibly related to the fact that the size of the Mg<sub>2</sub>Sn phase becomes much smaller and the amount

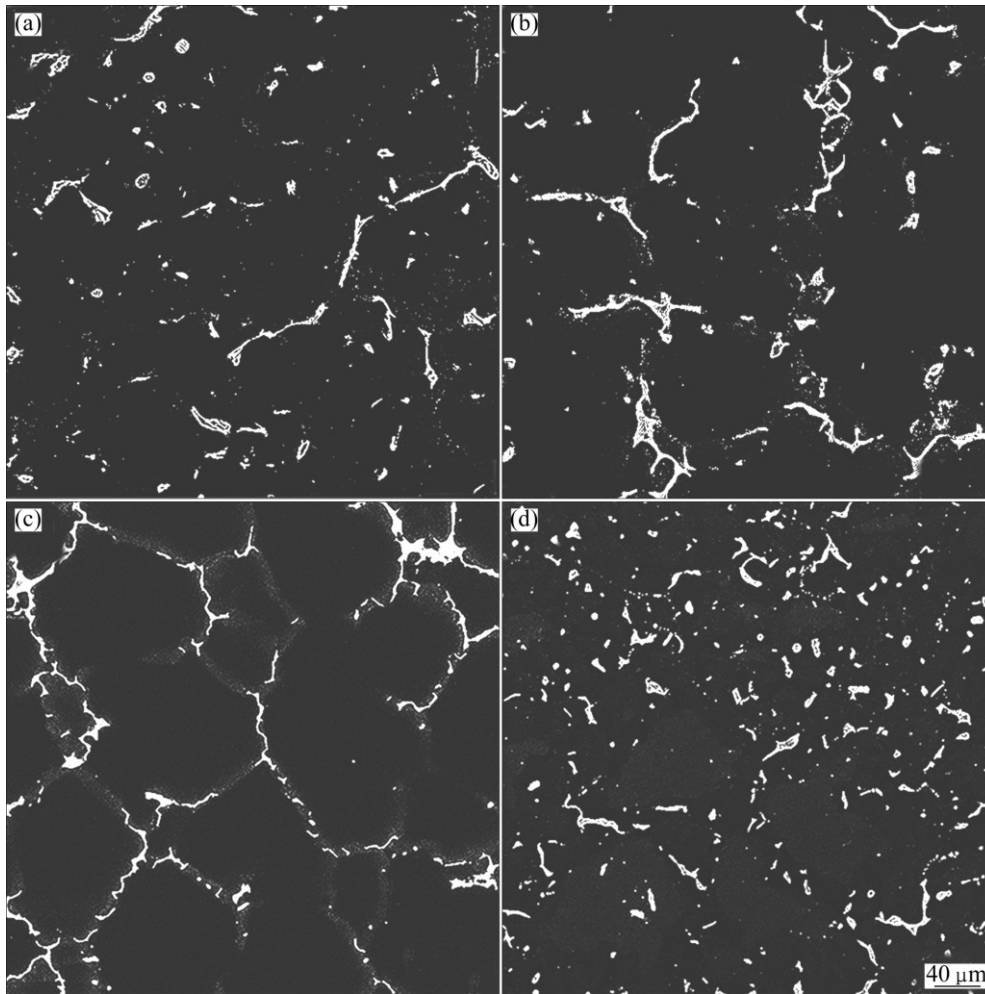


**Fig. 4** Low magnifications SEM images of as-cast microstructures of alloys with different ultrasonic treatment powers: (a) 0 W; (b) 300 W; (c) 500 W; (d) 700 W

decreases after 700 W ultrasonic treatment.

The ultrasonic treatment can induce energy loss of the sound wave, stir the melt and make the melt cool faster. Thus, the ultrasonic treatment can also generate streaming, which is a kind of forced convection generated in the melt. On the one hand, acoustic streaming can promote the heat transfer and element diffusion which is help to accelerate the remelting of dendrites at roots during the growth of the newly formed nuclei [18,23]. On the other hand, the second phases can also be fragmented under the impact force generated by bubbles collapsed. Therefore, the ultrasonic melt treatment can reduce the time of solidification, and the amount of alloy elements dissolved into the  $\alpha$ -Mg matrix increases, which suppresses the formation of the second phases and the second phases become discontinuous. Those are very likely the reasons why the small amount of  $Mg_2Sn$  phase cannot be found in the SEM images after 700 W ultrasonic treatment. As shown in Fig. 4(d), the morphologies of the phases which distribute at the grain boundaries are fine, discontinuous, uniform and

dispersive.

### 3.2 Mechanical properties

The tensile tests at room temperature were carried out to study the ultrasonic effects on the tensile properties of Mg–6Zn–0.5Y–2Sn alloy. Figure 6 shows the 0.2% tensile yield strength (YS), ultimate tensile strength (UTS) and fracture elongation of the alloys. As shown in Fig. 6, without ultrasonic treatment, the YS, UTS and elongation of the alloy at room temperature are 58 MPa, 189 MPa and 12.14%, respectively. When the ultrasonic treatment power increases to 700 W, the room temperature tensile properties of the alloy are significantly improved, in which the YS, UTS and fracture elongation are improved to 74 MPa, 246 MPa and 20.22%, respectively. Compared with the untreated alloy, the YS, UTS and elongation of the alloy are improved by 28%, 30% and 67%, respectively. It can be seen from Fig. 6 that the UTS of the alloy increases monotonously when the ultrasonic power increases from 0 to 700 W. However, compared with the alloy with

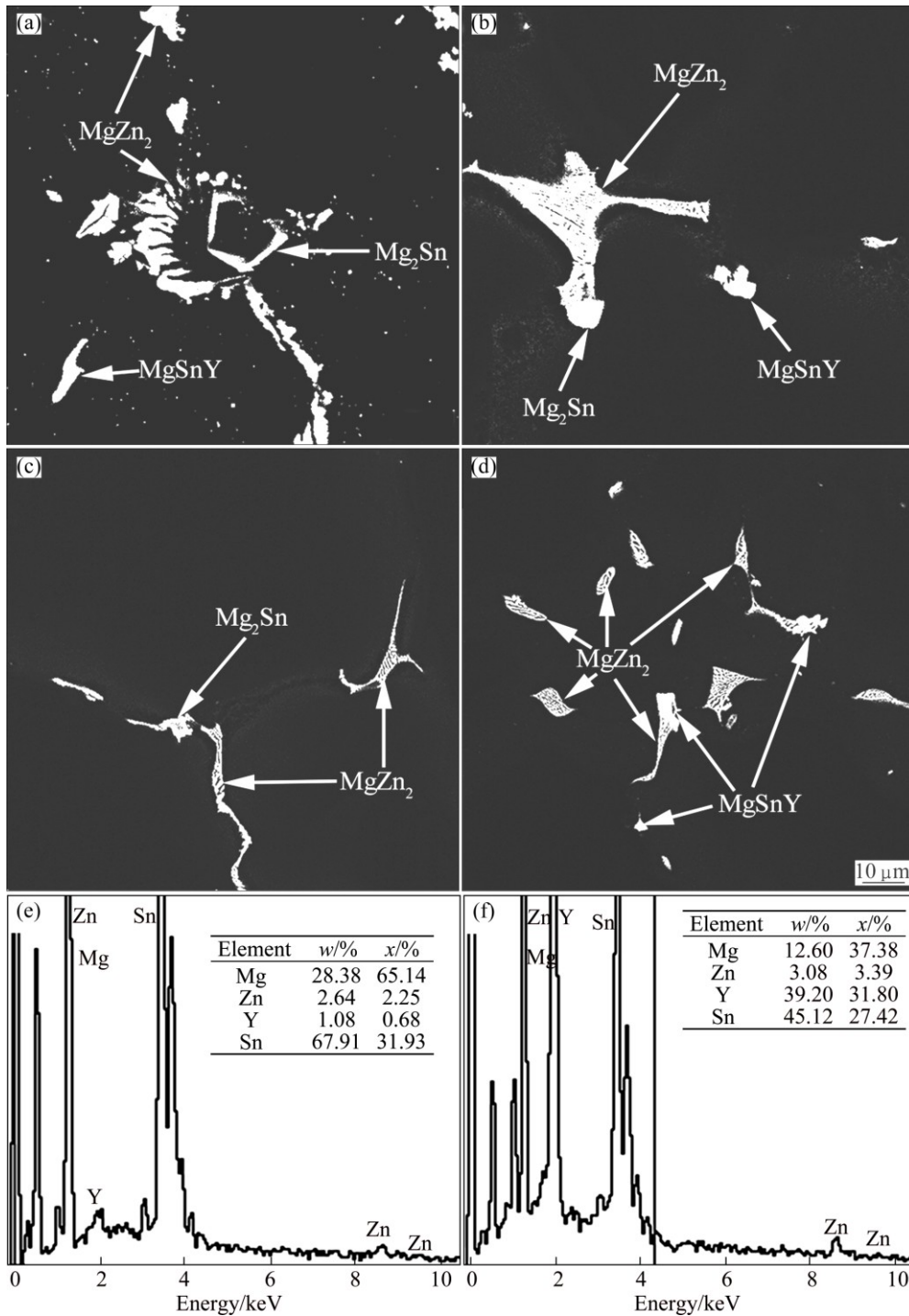


**Fig. 5** High magnifications SEM images of as-cast microstructures of alloys with different ultrasonic treatment powers of 0 W (a), 300 W (b), 500 W (c) and 700 W (d), and EDS results of  $Mg_2Sn$  phase (e) and  $MgSnY$  phase (f)

300 W ultrasonic power treatment, the elongation of the alloy with 500 W ultrasonic power treatment does not change obviously. Furthermore, although the UTS and elongation are not the best, the YS increases to the maximum when the ultrasonic power is 500 W. The exact reasons for this abnormal result are not completely clear now. These questions are subjects for further study in our group.

Actually, the effects of ultrasonic treatment on the tensile properties of alloys can be further confirmed from Fig. 7. Figure 7 shows the SEM images of tensile fracture morphologies of the as-cast alloys with different ultrasonic treatment powers failed in the tensile tests at room temperature. As shown in Fig. 7, a number of cleavage planes and steps can be observed, and several river patterns can also be seen on the tensile fracture

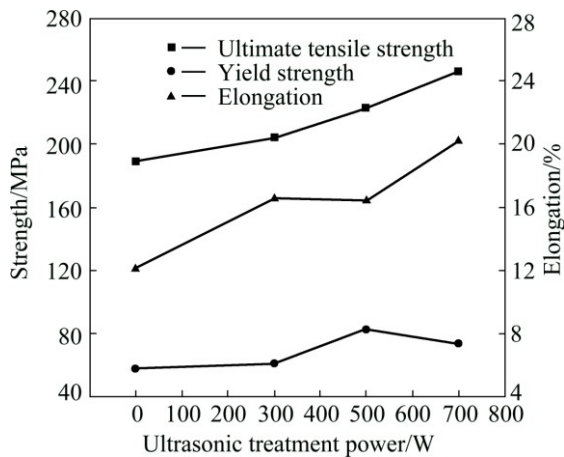


**Fig. 6** Tensile properties of Mg-6Zn-0.5Y-2Sn alloy with different ultrasonic treatment powers tested at room temperature

surface of alloys, which indicates that all fracture surfaces have mixed characteristics of cleavage and quasi-cleavage fractures [24]. Furthermore, compared with the alloy without ultrasonic treatment, after the ultrasonic treatment, the amount of plastic dimples

increases and some tear ridges can also be observed in Figs. 7(b)–(d). In addition, when the ultrasonic treatment power increases to 700 W, the amount of plastic dimples comes to the maximum. It is well known that cracks are more easily initiated and formed at the big secondary phases. Therefore, the coarse and irregular blocky MgSnY and Mg<sub>2</sub>Sn phases likely become the crack sources.

In summary, the improvement of mechanical properties of the Mg-6Zn-0.5Y-2Sn alloy with the ultrasonic treatment can be mainly attributed to two aspects: 1) with the application of the ultrasonic, nearly roundish equiaxed grains are achieved, which would significantly lead to the improvement of the ultimate tensile strength and elongation; 2) the Mg-Sn-Zn-Y quaternary alloys possess several stable intermetallic compounds, such as MgZn<sub>2</sub>, MgSnY and Mg<sub>2</sub>Sn phases, which can provide strong bonding with the matrix. It is clear that tensile properties depend directly on the microstructures, particle sizes and morphologies of reinforcement phases. After ultrasonic treatment, the coarse, semicontinuous, and non-uniform MgZn<sub>2</sub>, MgSnY, and Mg<sub>2</sub>Sn phases which distribute at the  $\alpha$ -Mg

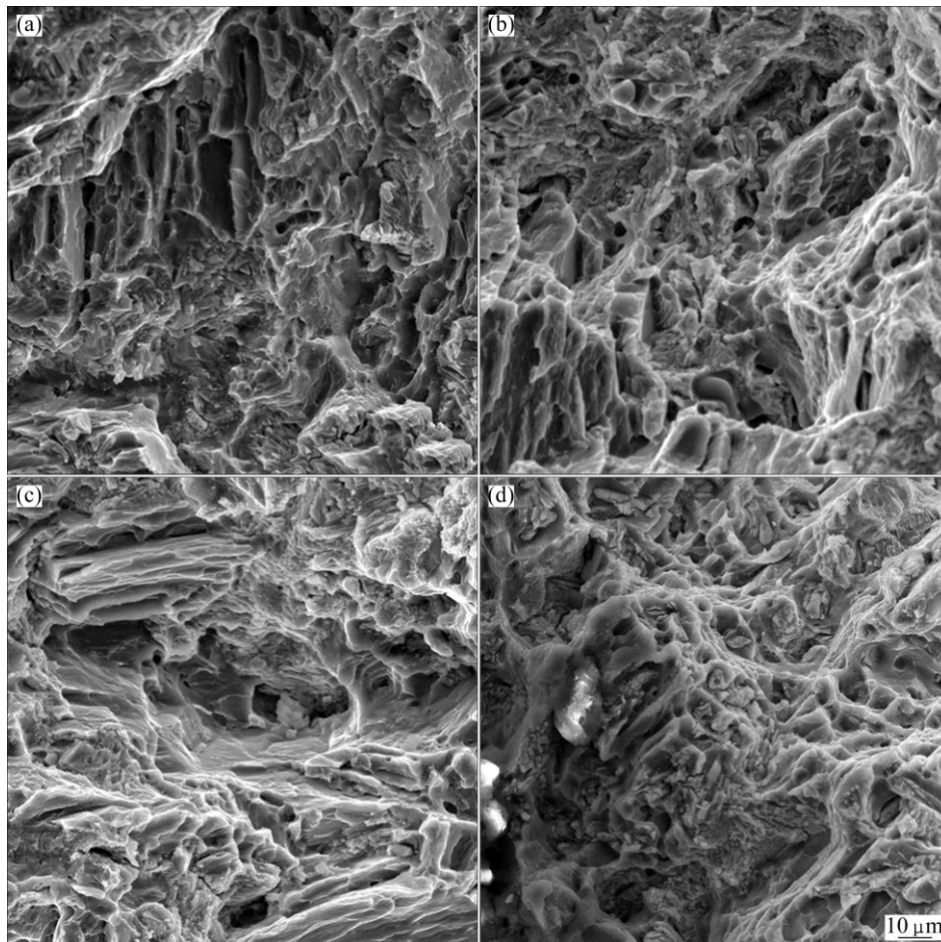


**Fig. 7** SEM images of tensile fracture morphologies of as-cast alloys with different ultrasonic treatment powers: (a) 0 W; (b) 300 W; (c) 500 W; (d) 700 W

boundaries are modified into fine, discontinuous, uniform and dispersive particles. Generally, the fine, discontinuous, uniform and dispersive particles are beneficial to dispersion strengthening which determines the tensile properties significantly. On the other hand, the fine and dispersive second phases are beneficial to the enhanced plasticity of alloy due to the fact that they have little constraint on the  $\alpha$ -Mg matrix and cannot make the formation of cracks easily.

## 4 Conclusions

1) The Mg–6Zn–0.5Y–2Sn alloy is mainly composed of primary  $\alpha$ -Mg, MgZn<sub>2</sub>, MgSnY, Mg<sub>2</sub>Sn and a small amount of I-phase. Although ultrasonic treatment has no obvious effect on the phase composition, the size, fraction and distribution of the intermetallic phases change appreciably.

2) The as-cast microstructure of the Mg–6Zn–0.5Y–2Sn alloy is improved after ultrasonic treatment. When the ultrasonic treatment is applied on the solidification process of the alloy, the coarse dendrites gradually change to roundish equiaxed grains with increasing the ultrasonic treatment power.

3) MgZn<sub>2</sub>, MgSnY, and Mg<sub>2</sub>Sn phases in the Mg–6Zn–0.5Y–2Sn alloy without ultrasonic treatment are coarse, semicontinuous and non-uniform. After the ultrasonic treatment, the phases which distribute at the grain boundaries become fine, discontinuous, uniform and dispersive.

4) The mechanical properties of the Mg–6Zn–0.5Y–2Sn alloy with ultrasonic treatment increase significantly. Compared with the untreated alloy, the ultimate tensile strength and elongation of the alloy with 700 W ultrasonic treatment improve from 189 MPa and 12.14% to 246 MPa and 20.22%, which are improved by 30% and 67%, respectively. Besides, after 500 W ultrasonic treatment, the 0.2% tensile yield strength improves from 58 to 83 MPa, which is improved by 43%.

## References

- [1] ELIEZER D, AGHION E, FROES F H. Magnesium science, technology and applications [J]. *Advanced Performance Materials*, 1998, 5(3): 201–212.
- [2] YANG M B, LI H L, DUAN C Y, ZHANG J. Effects of minor Ti addition on as-cast microstructure and mechanical properties of Mg–3Sn–2Sr (wt.%) magnesium alloy [J]. *Journal of Alloys and Compounds*, 2013, 579(1): 92–99.
- [3] YANG Z, LI J P, ZHANG J X, LORIMER G W, ROBSON J. Review on research and development of magnesium alloys [J]. *Acta Metallurgica Sinica*, 2008, 21(5): 313–328.
- [4] WANG J F, GAO S, SONG P F, HUANG X F, SHI Z Z, PAN F S. Effects of phase composition on the mechanical properties and damping capacities of as-extruded Mg–Zn–Y–Zr alloys [J]. *Journal of Alloys and Compounds*, 2011, 509(34): 8567–8572.
- [5] LUO A A. Recent magnesium alloy development for elevated temperature applications [J]. *International Materials Reviews*, 2004, 49(1): 13–30.
- [6] QI F G, ZHANG D F, ZHANG X H, PAN F S. Effect of Y addition on microstructure and mechanical properties of Mg–Zn–Mn alloy [J]. *Transactions of Nonferrous Metals Society of China*, 2014, 24(5): 1352–1364.
- [7] MORA E, GARCES G, ONORBE E, PEREZ P, ADEVA P. High-strength Mg–Zn–Y alloys produced by powder metallurgy [J]. *Scripta Materialia*, 2009, 60(9): 776–779.
- [8] ASGHARZADEH H, YOON E Y, CHAE H J, KIM T S, LEE J W, KIM H S. Microstructure and mechanical properties of a Mg–Zn–Y alloy produced by a powder metallurgy route [J]. *Journal of Alloys and Compounds*, 2014, 586(S1): s95–s100.
- [9] ZHANG Y, ZENG X Q, LIU L F, LU C, ZHOU H T, LI Q, ZHU Y P. Effects of yttrium on microstructure and mechanical properties of hot-extruded Mg–Zn–Y–Zr alloys [J]. *Materials Science and Engineering A*, 2004, 373(1–2): 320–327.
- [10] DONG X G, FU J W, WANG J, YANG Y S. Microstructure and tensile properties of as-cast and as-aged Mg–6Al–4Zn alloys with Sn addition [J]. *Materials and Design*, 2013, 51: 567–574.
- [11] TUREN Y. Effect of Sn addition on microstructure, mechanical and casting properties of AZ91 alloy [J]. *Materials and Design*, 2013, 49: 1009–1015.
- [12] QI F G, ZHANG D F, ZHANG X H, XU X X. Effect of Sn addition on the microstructure and mechanical properties of Mg–6Zn–1Mn(wt.%) alloy [J]. *Journal of Alloys and Compounds*, 2014, 585: 656–666.
- [13] HUANG S, WANG J F, HOU F, LI Y, PAN F S. Effect of Sn on the formation of the long period stacking ordered phase and mechanical properties of Mg–RE–Zn alloy [J]. *Materials Letters*, 2014, 137: 143–146.
- [14] GORNY A, BAMBERGER M, KATSMAN A. High temperature phase stabilized microstructure in Mg–Zn–Sn alloys with Y and Sb additions [J]. *Journal of Materials Science*, 2007, 42(24): 10014–10022.
- [15] ZHAO H D, QIN G W, REN Y P, PEI W L, GUO Y. Isothermal sections of the Mg-rich corner in the Mg–Sn–Y ternary system at 300 and 400 °C [J]. *Journal of Alloys and Compounds*, 2009, 481(1–2): 140–143.
- [16] HU G S, ZHANG D F, ZHAO D Z, SHEN X, JIANG L Y, PAN F S. Microstructures and mechanical properties of extruded and aged Mg–Zn–Mn–Sn–Y alloys [J]. *Transactions of Nonferrous Metals Society of China*, 2014, 24(10): 3070–3075.
- [17] ESKIN G I. Broad prospects for commercial application of the ultrasonic (cavitation) melt treatment of light alloys [J]. *Ultrasonics Sonochemistry*, 2001, 8(3): 319–325.
- [18] YAO L, HAO H, JI S H, FANG C F, ZHANG X G. Effects of ultrasonic vibration on solidification structure and properties of Mg–8Li–3Al Alloy [J]. *Transactions of Nonferrous Metals Society of China*, 2011, 21(6): 1241–1246.
- [19] LIU X B, OSAWA Y, TAKAMORI S, MUKAI T. Microstructure and mechanical properties of AZ91 alloy produced with ultrasonic vibration [J]. *Materials Science and Engineering A*, 2008, 487(1–2): 120–123.
- [20] ZHANG Z Q, LE Q C, CUI J Z. Ultrasonic treatment of magnesium alloy melts and its effects on solidification microstructures [J]. *Materials Science Forum*, 2007, 546–549: 129–132.
- [21] WANG Zhao-hui, WANG Xu-dong, WANG Qing-feng, DU Wen-bo. Effects of ultrasonic treatment on microstructure and mechanical properties of Mg–5Zn–2Er alloy [J]. *Transactions of Nonferrous Metals Society of China*, 2011, 21(4): 773–777.

- [22] JIAN X, XU H, MEEK T T, HAN Q. Effect of power ultrasound on solidification of aluminum A356 alloy [J]. Materials Letters, 2005, 59(2–3): 190–193.
- [23] GAO D, LI Z, HAN Q, ZHAI Q. Effect of ultrasonic power on microstructure and mechanical properties of AZ91 alloy [J]. Materials Science and Engineering A, 2009, 502(1–2): 2–5.
- [24] YANG Ming-bo, ZHANG Jia, GUO Ting-zhang. Effects of Ca addition on as-cast microstructure and mechanical properties of Mg–3Ce–1.2Mn–1Zn (wt.%) magnesium alloy [J]. Materials and Design, 2013, 52: 274–283.

## 超声处理对 Mg–6Zn–0.5Y–2Sn 合金 显微组织及力学性能的影响

薛寒松<sup>1,2</sup>, 邢志辉<sup>1</sup>, 张维娜<sup>1</sup>, 杨钢<sup>1</sup>, 潘复生<sup>1,2</sup>

1. 重庆大学 材料科学与工程学院, 重庆 400044;
2. 重庆大学 国家镁合金材料工程技术研究中心, 重庆 400044

**摘 要:** 研究超声处理对 Mg–6Zn–0.5Y–2Sn 合金显微组织及力学性能的影响。结果表明, 超声处理对 Mg–6Zn–0.5Y–2Sn 合金显微组织及力学性能有显著影响。Mg–6Zn–0.5Y–2Sn 合金是由  $\alpha$ -Mg 相、MgZn<sub>2</sub> 相、MgSnY 相、Mg<sub>2</sub>Sn 相和少量 I 相组成。经超声处理后, I 相基本消失, 并且随着超声功率的提高, 粗大的枝晶结构逐渐变成圆整的等轴晶, 位于晶界附近粗大、半连续、不均匀分布的第二相逐渐变得细小、不连续、均匀且弥散分布。当超声功率达到 700 W 时, Mg–6Zn–0.5Y–2Sn 合金的综合力学性能达到最佳。与未超声处理的镁合金相比, 其屈服强度、极限抗拉强度和伸长率分别提高了 28%、30% 和 67%。

**关键词:** Mg–6Zn–0.5Y–2Sn 合金; 超声处理; 显微组织; 力学性能

(Edited by Mu-lan QIN)